
TURING PATTERNS IN A LESLIE-GOWER PREDATOR PREY MODEL

A PREPRINT

F. Capone^{a*}
fcapone@unina.it

R. De Luca^a
roberta.deluca@unina.it

I. Torcicollo^b
i.torcicollo@iac.cnr.it

^aDipartimento di Matematica e Applicazioni "R.Caccioppoli"
Università degli Studi di Napoli Federico II
Via Cintia, Monte S. Angelo, 80126 Napoli
Italy

^bIstituto per le Applicazioni del Calcolo "Mauro Picone", CNR
Via Pietro Castellino, 80129 Napoli
Italy

February 8, 2023

Abstract

A reaction-diffusion Leslie-Gower predator-prey model, incorporating the fear effect and prey refuge, with Beddington-DeAngelis functional response, is introduced. A qualitative analysis of the solutions of the model and the stability analysis of the coexistence equilibrium, are performed. Sufficient conditions guaranteeing the occurrence of Turing instability have been determined either in the case of self-diffusion or in the case of cross-diffusion. Different types of Turing patterns, representing a spatial redistribution of population in the environment, emerge for different values of the model parameters.

Keywords Population dynamics · Predator-Prey · Turing instability · Cross-Diffusion · Turing patterns · Reaction-Diffusion

1 Introduction

Predator-prey models describe the interaction between two population in which a species (the predators) sustains its self by eating another one (the prey). Starting from the pioneering Lotka-Volterra predator-prey model, different generalizations have been proposed in order to overcome some criticalities and better describe some real situations [1, 2, 3, 4, 5, 6, 7, 8], [9, 10]. In particular, a Leslie-Gower model has been successively formulated in order to introduce an asymptotic limit to the growth of both populations (not recognized by the classical model) [11, 12, 13, 14]. This model consists in two ordinary differential equations in which the environmental carrying capacity of predators depends on the ratio between the two population densities. A fundamental role in mathematical modeling of predator-prey dynamics, is played by the functional response defined as the number of prey consumed by one predator per unit of time. The functional response depends on a number of factors such as the prey's ability to escape an attack or the predator's search efficiency. Holling [15] proposed three functional responses depending only on the number of prey (N). In particular, the Holling functionals are:

*Corresponding author.

- Type I: $\mathcal{F} = mN$;
- Type II: $\mathcal{F} = \frac{mN}{a + N}$;
- Type III: $\mathcal{F} = \frac{mN^2}{a + N^2}$

being a, m constants. The choice of the functional response depends on the different predation behaviour to be modeled. In particular, the type I is used when there is no handling time of the captured prey and population densities are not too large. Type II introduces a maximum predation rate to describe the situation in which predators can feel satiated when there is abundant available food. Type III describes the increasing of predators search activity with increasing prey density. However, there are some circumstances in which a functional response, depending of both population densities, should be used. This is the case, for example, in which predators behavior affects the prey dynamics. Beddington-DeAngelis [16, 17] proposed a functional response which comes from a generalization of the Holling type II functional response, introducing at the denominator an additive linear term depending on the predators number to model the mutual interference between predators. In [18] a modified Leslie-Gower model has been introduced to describe the predator-prey interaction by considering a Beddington-DeAngelis functional response and taking into account of two important aspects: the fear effect and the prey refuge. Fear may have important consequences on the ecosystem [19, 20, 21, 22]. For example, in [19] it has been observed that some birds female, that experienced frequent nests predation, produce fewer eggs in the subsequent nests. In order to model this phenomenon, the natural birth rate of preys is multiplied by a function $f(k, P)$ depending on the level of fear k and on the predators density P such as:

- 1) in the absence of fear or in the absence of predators, the function is equal to 1, meaning that the natural birth rate of preys is constant

$$f(0, P) = 1, \quad f(k, 0) = 1$$

- 2) when the level of fear or the predators density is huge, the function f tends to zero

$$\lim_{k \rightarrow \infty} f(k, P) = 0, \quad \lim_{P \rightarrow \infty} f(k, P) = 0$$

- 3) the function f has to be decreasing with respect to k and P

$$\frac{\partial f(k, P)}{\partial k} < 0, \quad \frac{\partial f(k, P)}{\partial P} < 0.$$

In time of predation, preys can experience hiding behavior [23], [24], [25]. Then, introducing a parameter $\eta \in [0, 1]$ representing the fraction of prey protected by predation, denoting by N the number of prey, $\eta(1 - N)$ is the number of prey outside of protection. The model introduced in [18] considers the case in which both populations are homogeneously mixed in the environment. The biologically meaningful equilibria have been determined and sufficient conditions guaranteeing the linear stability of the coexistence equilibrium have been found.

In order to generalize the results obtained in [18], in this paper we consider the case in which populations are heterogeneously mixed in the environment to incorporate a random movement of both species. Such model better describes, for example, the situations in which predators can move to search for preys and these ones can move to escape by predators attack. When diffusion is incorporated in the mathematical model, a spatial distribution, periodic in space and constant in time, of both populations can be observed under certain conditions (see [26] and the references therein). In fact, it is possible to look for conditions guaranteeing that an equilibrium, stable in the absence of diffusion, becomes unstable when diffusion is allowed. The diffusion-driven instability is called Turing instability and has been widely studied in literature, especially to investigate for the Turing patterns formation ([27]). This approach can be extended to other interacting models with different functional responses, and also in other fields of applied mathematics where nonlinear mathematical models having a similar structure are considered ([28, 29, 30, 31]). The simplest diffusion is the linear one, meaning that the time evolution of one species is affected by the random movement of the same species. In [32] a modified Leslie-Gower model is introduced. It is assumed a linear constant self diffusion and conditions guaranteeing the onset of Turing, Hopf, Turing-Hopf bifurcations, is investigated. However, more sophisticated diffusion terms can be introduced due to the fact that the interaction between population affects each other's behaviour. Among these, the cross-diffusion terms are introduced when the behaviour of one species depends on the random movements of both species.

The plan of the paper is as follows. Section 2 is devoted to the introduction of the mathematical model which consists of two reaction-diffusion equations governing the evolution of predators and prey interactions. A simple linear, constant, self-diffusion is introduced for both the species. Section 3 is devoted to a qualitative analysis of the solutions: the boundedness and existence of absorbing sets (i.e. positively invariant and attractive sets) in the phase space are explored. In the subsequent Section 4, the existence of biologically meaningful equilibria is analyzed. Section 5 deals with the linear instability of the coexistence equilibrium. Precisely, in Subsection 5.1, the linear instability in the homogeneous case is investigated. The heterogeneous case is examined in Subsection 5.2 where sufficient conditions guaranteeing the occurrence of Turing instability, have been determined. Since the set of parameters verifying the conditions for the diffusion-driven instability is very strict, in Section 6 the model introduced in Section 2, has been generalized to take into account of cross-diffusion and conditions guaranteeing the onset of Turing instability have been determined in the case in which this kind of instability is not observable when the self-diffusion is considered. In Section 7 the amplitude equations are obtained. Section 8 deals with numerical simulations in order to explore a richer dynamic of population interactions showing that, under certain conditions, spatial patterns emerge. The paper ends with a Conclusion section (Section 9) collecting all the obtained results.

2 Mathematical model

In [18], a Leslie-Gower predator-prey model with Beddington-DeAngelis functional response, incorporating fear effect and prey refuge, has been analyzed. Denoting by N and P the number of prey and predators, respectively, the model introduced in [18] is

$$\begin{cases} \frac{dN}{dt} = \left(\frac{r_1}{1+kP} - qN - \frac{\alpha(1-\eta)P}{a+b(1-\eta)N+cP} - d \right) N, \\ \frac{dP}{dt} = \left(r_2 - \frac{\beta P}{(1-\eta)N+\gamma} \right) P \end{cases} \quad (1)$$

with r_1, r_2 birth rates of prey and predator population, q, β competition rates of prey and predators; α reduction rate of prey into predators, a, γ environmental protects of prey and predators, b, c constants, d natural death rate of prey, $\eta \in [0, 1[$ measures the protection of prey (i.e. η is the number of prey protected by predation), k rate of fear expressing the anti-predator behaviour in prey. All the constants appearing in (1) are positive. In model (1), population is considered homogeneously mixed in the environment (i.e. diffusion is neglected). In order to generalize model (1) to the most significant case in which both species can randomly move in the environment (for example, prey can escape from regions with high risk of predation, or predators can move for searching food), we introduce – at the first – the simplest diffusion, i.e. the linear, constant self-diffusion terms, to obtain

$$\begin{cases} \frac{\partial N}{\partial \tau} = \left(\frac{r_1}{1+kP} - qN - \frac{\alpha(1-\eta)P}{a+b(1-\eta)N+cP} - d \right) N + d_1 \Delta N, \\ \frac{\partial P}{\partial \tau} = \left(r_2 - \frac{\beta P}{(1-\eta)N+\gamma} \right) P + d_2 \Delta P \end{cases} \quad (2)$$

where d_i are positive constants ($i = 1, 2$), denoting the diffusion coefficients and Δ is the spatial Laplacian operator. In the sequel, we denote by Ω the domain in which species can spread, assuming that Ω is a regular domain, and associate to (2) smooth positive initial data:

$$N(\mathbf{X}, 0) = N_0(\mathbf{X}), \quad P(\mathbf{X}, 0) = P_0(\mathbf{X}), \quad \mathbf{X} \in \Omega \quad (3)$$

and homogeneous Neumann boundary conditions (no-flux)

$$\nabla N \cdot \mathbf{n} = 0, \quad \nabla P \cdot \mathbf{n} = 0, \quad \text{on } \partial\Omega \times \mathbb{R}^+, \quad (4)$$

being \mathbf{n} the outward unit normal to the boundary $\partial\Omega$. Introducing the transformation (see [18])

$$\begin{cases} \mathbf{x} = \frac{\mathbf{X}}{L}, \quad t = r_2 \tau, \quad n = \frac{qN}{r_2}, \quad p = \frac{qP}{br_2^2}, \quad \mu = \frac{r_1}{r_2}, \quad \rho = \frac{kbr_2^2}{q}, \\ \delta = \frac{q}{r_2}, \quad \sigma = \frac{br_2}{aq}, \quad \Phi = \frac{\alpha br_2}{aq}, \quad \xi = \frac{bcr_2^2}{aq}, \quad \theta = b\beta, \quad \nu = \frac{\gamma q}{r_2} \end{cases} \quad (5)$$

with L being the Ω -diameter, setting $\gamma_i = \frac{d_i}{r_i L^2}$, ($i = 1, 2$), model (2) becomes

$$\begin{cases} \frac{\partial n}{\partial t} = \left(\frac{\mu}{1+\rho p} - n - \frac{(1-\eta)\Phi p}{1+\sigma(1-\eta)n+\xi p} - \delta \right) n + \gamma_1 \Delta n, \\ \frac{\partial p}{\partial t} = \left(1 - \frac{\theta}{(1-\eta)n+\nu} \right) p + \gamma_2 \Delta p \end{cases} \quad (6)$$

under the initial-boundary conditions

$$\begin{aligned} n(\mathbf{x}, 0) &= \mathbf{n}_0(\mathbf{x}), \quad p(\mathbf{x}, 0) = p_0(\mathbf{x}), \quad \mathbf{x} \in \Omega, \\ \nabla n \cdot \mathbf{n} &= 0, \quad \nabla p \cdot \mathbf{n} = 0, \quad \text{on } \partial\Omega \times \mathbb{R}^+. \end{aligned} \quad (7)$$

In the sequel we assume, accordingly to [18], that $\mu > \delta$.

3 Boundedness of solutions

In this section, we investigate the boundedness of solutions and the existence of absorbing sets in the phase space (i.e. positively invariant and attractive sets). Denote by $\|\cdot\|, \|\cdot\|_\infty$ the L^2 and L^∞ -norm. Let $T > 0$ be a fixed time and $\Omega_T = \Omega \times (0, T]$ be the parabolic cylinder. The following theorem holds true.

Theorem 1. *Let $(n, p) \in [C_1^2(\Omega_T) \cap C(\bar{\Omega}_T)]^2$ the non negative solution of (6)-(7). Then $\forall \varphi \in \{n, p\}$, φ is bounded a.e. in Ω according to*

$$n(\mathbf{x}, t) \leq C_\infty^{(1)}(n_0(\mathbf{x})) := M_1, \quad p(\mathbf{x}, t) \leq C_\infty^{(2)}(p_0(\mathbf{x})) := M_2, \quad (8)$$

where C_∞^i , ($i = 1, 2$) are positive constants depending on the initial data.

Proof. $n(\mathbf{x}, t)$ is a sub-solution of the problem

$$\begin{cases} \frac{\partial S_1}{\partial t} - \gamma_1 \Delta S_1 = (\mu - \delta - S_1)S_1, \\ \nabla S_1 \cdot \mathbf{n} = 0, \quad \text{on } \partial\Omega \times \mathbb{R}^+, \\ S_1(\mathbf{x}, 0) = S_1^0(\mathbf{x}) = \max_{\bar{\Omega}} n_0(\mathbf{x}). \end{cases} \quad (9)$$

Since

$$(\mu - \delta - S_1)S_1 \leq \frac{3}{2}S_1^2 + \frac{(\mu - \delta)^2}{2}, \quad (10)$$

in view of Theorem 1 of [33], one obtains that, denoting by $\tau_1(S_1^0)$ the maximal existence time of the solution $S_1(\mathbf{x}, t)$ of (9), since – from the continuous dependence on the initial data – there exists a positive constant $C_1(S_1^0)$ such that

$$\|S_1(\cdot, t)\| \leq C_1(S_1^0), \quad \forall t \in (0, \tau_1(S_1^0)), \quad (11)$$

the solution $S_1(\mathbf{x}, t)$ exists for all time and there exists a positive constant $C_\infty^{(1)}$ such that

$$\|S_1(\cdot, t)\|_\infty \leq C_\infty^{(1)}(S_1^0), \quad \forall t > 0. \quad (12)$$

Similarly, $p(\mathbf{x}, t)$ is a sub-solution of the problem

$$\begin{cases} \frac{\partial S_2}{\partial t} - \gamma_2 \Delta S_2 = \left(1 - \frac{\theta}{(1-\eta)M_1 + \nu}\right) S_2, \\ \nabla S_2 \cdot \mathbf{n} = 0, \quad \text{on } \partial\Omega \times \mathbb{R}^+, \\ S_2(\mathbf{x}, 0) = S_2^0(\mathbf{x}) = \max_{\bar{\Omega}} p_0(\mathbf{x}). \end{cases} \quad (13)$$

Since

$$\left(1 - \frac{\theta}{(1-\eta)M_1 + \nu}\right) S_2 \leq \left(1 - \frac{\theta}{(1-\eta)M_1 + \nu}\right)^2 \frac{S_2^2}{2} + \frac{1}{2}, \quad (14)$$

in view of Theorem 1 of [33], one obtains that, denoting by $\tau_2(S_2^0)$ the maximal existence time of the solution $S_2(\mathbf{x}, t)$ of (13), since – from the continuous dependence on the initial data – there exists a positive constant $C_2(S_2^0)$ such that

$$\|S_2(\cdot, t)\| \leq C_2(S_2^0), \quad \forall t \in (0, \tau_2(S_2^0)), \quad (15)$$

the solution $S_2(\mathbf{x}, t)$ exists for all time and there exists a positive constant $C_\infty^{(2)}$ such that

$$\|S_2(\cdot, t)\|_\infty \leq C_\infty^{(2)}(S_2^0), \quad \forall t > 0 \quad (16)$$

and the thesis is proved.

Theorem 2. $\forall \varepsilon > 0$ the manifold

$$\Sigma_\varepsilon = \left\{ (n, p) \in [\mathbf{R}^+]^2 : \|n\|^2 + \|p\|^2 \leq (1 + \varepsilon) \frac{\bar{a}}{\delta} \right\} \quad (17)$$

with

$$\bar{a} = 2|\Omega| [(\sigma + 1)M_1^2 + M_1C_\infty^2(1 + \alpha C_\infty)], \quad (18)$$

is an absorbing set for system (6).

Proof. Multiplying (6)₁ by n , (6)₂ by p , adding the resulting equations and integrating over Ω , by virtue of the divergence theorem, the boundary conditions (7)₂ and (8), it turns out that

$$\frac{1}{2} \frac{d(\|n\|^2 + \|p\|^2)}{dt} \leq -\delta(\|n\|^2 + \|p\|^2) + \bar{a}, \quad (19)$$

with $\bar{a} = \left(M_1^3 + (1 - \eta)\Phi M_1^2 M_2 + \mu M_1^2 \beta + \frac{\theta}{2} M_2^2 + (1 + \delta) M_2^2 \right) |\Omega|$. Then, setting $E = \|n\|^2 + \|p\|^2$, it follows that

$$\frac{dE}{dt} \leq -2\delta E + 2\bar{a}. \quad (20)$$

Following the procedure in [34], one can prove that Σ is an absorbing set.

4 Biologically meaningful equilibria: existence and a priori estimates

The biologically meaningful equilibria are the positive solutions of the system

$$\begin{cases} \left(\frac{\mu}{1 + \rho p} - n - \frac{(1 - \eta)\Phi p}{1 + \sigma(1 - \eta)n + \xi p} - \delta \right) n + \gamma_1 \Delta n = 0, \\ \left(1 - \frac{\theta}{(1 - \eta)n + \nu} \right) p + \gamma_2 \Delta p = 0. \end{cases} \quad (21)$$

The following Theorem holds true.

Theorem 3. Let $0 < \gamma \leq \min\{\gamma_1, \gamma_2\}$. Then there exist positive constants $C_i(\gamma)$ ($i = 1, 2$) depending on the positive constants appearing in (6) and Ω such that any positive solution of (21) verifies:

$$\begin{aligned} \max_{\bar{\Omega}} n(\mathbf{x}) &\leq M_1, & \max_{\bar{\Omega}} p(\mathbf{x}) &\leq M_2, \\ \frac{\max_{\bar{\Omega}} n(\mathbf{x})}{\min_{\bar{\Omega}} n(\mathbf{x})} &\leq C_1(\gamma), & \frac{\max_{\bar{\Omega}} p(\mathbf{x})}{\min_{\bar{\Omega}} p(\mathbf{x})} &\leq C_2(\gamma). \end{aligned} \quad (22)$$

Proof. Inequalities (22)₁, (22)₂ follow easily from (8). In view of the Harnack inequality, (22)₃, (22)₄ are obtained.

Let us set α_1 the lowest positive eigenvalue of the spectral problem

$$\begin{cases} \Delta \varphi = -\alpha \varphi, & \text{in } \Omega \\ \nabla \varphi \cdot \mathbf{n} = 0, & \text{on } \partial\Omega \times \mathbb{R}^+ \end{cases} \quad (23)$$

and

$$\bar{\varphi} = \frac{1}{|\Omega|} \int_{\Omega} \varphi d\Omega, \quad \forall \varphi \in \{n, p\}. \quad (24)$$

The following theorem provides a sufficient condition for the non-existence of non-constant solutions of (21).

Theorem 4. If

$$\begin{cases} \gamma_1 \geq \frac{C_1(\gamma)}{2\alpha_1} \{ \mu \rho + (1 - \eta)\Phi + \sigma(1 - \eta)^2 \Phi [M_1 + M_2] \}, \\ \gamma_2 \geq \frac{C_2(\gamma)\theta(1 - \eta)}{4\mu^2\alpha_1} \{ \mu \rho + (1 - \eta)\Phi + \sigma(1 - \eta)^2 \Phi M_1 + 1 \}, \end{cases} \quad (25)$$

holds, then system (21) does not admit any positive non constant solution.

Proof. Let (n, p) be a positive solution of (21). Multiplying (21)₁ by $\frac{n - \bar{n}}{n}$, (21)₂ by $\beta \frac{p - \bar{p}}{p}$, integrating over Ω and adding the resulting equations, one obtains – in view of the divergence theorem and the boundary conditions (7)₂

$$\begin{aligned}
& \gamma_1 \int_{\Omega} \bar{n} \frac{(\nabla n)^2}{n^2} d\Omega + \beta \gamma_2 \int_{\Omega} \bar{p} \frac{(\nabla p)^2}{p^2} d\Omega = -\mu \rho \int_{\Omega} \frac{(n - \bar{n})(p - \bar{p})}{(1 + \rho p)(1 + \rho \bar{p})} d\Omega \\
& - \|n - \bar{n}\|^2 - (1 - \eta) \Phi \int_{\Omega} \frac{(n - \bar{n})(p - \bar{p})}{[1 + \sigma(1 - \eta)n + \xi p][1 + \sigma(1 - \eta)\bar{n} + \xi \bar{p}]} d\Omega \\
& - \sigma(1 - \eta)^2 \Phi \bar{n} \int_{\Omega} \frac{(n - \bar{n})(p - \bar{p})}{[1 + \sigma(1 - \eta)n + \xi p][1 + \sigma(1 - \eta)\bar{n} + \xi \bar{p}]} d\Omega \\
& + \sigma(1 - \eta)^2 \Phi \bar{p} \int_{\Omega} \frac{(n - \bar{n})(p - \bar{p})}{[1 + \sigma(1 - \eta)n + \xi p][1 + \sigma(1 - \eta)\bar{n} + \xi \bar{p}]} d\Omega \\
& + \theta \beta (1 - \eta) \int_{\Omega} \frac{(n - \bar{n})(p - \bar{p})}{[(1 - \eta)n + \nu][(1 - \eta)\bar{n} + \nu]} d\Omega.
\end{aligned} \tag{26}$$

Applying the Poincaré inequality and (22)₃–(22)₄, one recovers that

$$\gamma_1 \int_{\Omega} \bar{n} \frac{(\nabla n)^2}{n^2} d\Omega + \beta \gamma_2 \int_{\Omega} \bar{p} \frac{(\nabla p)^2}{p^2} d\Omega \geq \frac{\alpha_1 \gamma_1}{C_1(\gamma)} \|n - \bar{n}\|^2 + \frac{\alpha_1 \beta \gamma_2}{C_2(\gamma)} \|p - \bar{p}\|^2. \tag{27}$$

Substituting (27) in (26), in view of (22)₁–(22)₂, choosing $\beta = \frac{2\nu^2}{\theta(1 - \eta)}$, one has that

$$\begin{aligned}
& \frac{\alpha_1 \gamma_1}{C_1(\gamma)} \|n - \bar{n}\|^2 + \frac{\alpha_1 \beta \gamma_2}{C_2(\gamma)} \|p - \bar{p}\|^2 \leq \\
& \leq [\mu \rho + (1 - \eta) \Phi + \sigma(1 - \eta)^2 \Phi M_1 + 2\sigma(1 - \eta)^2 \Phi M_2] \frac{\|n - \bar{n}\|^2}{2} \\
& + [\mu \rho + (1 - \eta) \Phi + \sigma(1 - \eta)^2 \Phi M_1 + 2] \frac{\|p - \bar{p}\|^2}{2}
\end{aligned} \tag{28}$$

that is impossible when (25) holds.

In the sequel we assume that (25) holds and hence (6) admits only the constant steady states found in [18], i.e.:

- $E_0 = (0, 0)$, representing the extinction of both species;
- $E_1 = (\mu - \delta, 0)$, the prey-only equilibrium;
- $E_2 = (0, \nu/\theta)$, the predator-only equilibrium;
- $E_* = (n_*, p_*)$, the coexistence equilibrium, with $p_* = \frac{(1 - \eta)n_* + \nu}{\theta}$ and n_* positive solution of

$$U_1 n_*^3 + U_2 n_*^2 + U_3 n_* + U_4 = 0, \tag{29}$$

where

$$\begin{aligned}
U_1 &= \rho(1 - \eta)^2(\xi + \sigma\theta), \\
U_2 &= (1 - \eta)\rho\nu(2\xi + \sigma\theta) + (1 - \eta)\{(1 - \eta)[\delta\rho\theta + \delta\rho\xi + \Phi\rho(1 - \eta)] + \\
& \quad + \sigma\theta^2 + \rho\theta + \xi\theta\} > 0, \\
U_3 &= \nu^2\rho\xi + \nu\{(1 - \eta)[\delta\rho\sigma\theta + 2\delta\rho\xi + 2\Phi\rho(1 - \eta)] + \theta\rho + \theta\xi\} + \\
& \quad + \theta\{(1 - \eta)[(\xi + \sigma\theta)(\delta - \mu) + \delta\rho] + \Phi(1 - \eta)^2 + \theta\}, \\
U_4 &= \nu^2\rho[\delta\xi + \Phi(1 - \eta)] + \theta\nu[\xi(\delta - \mu) + \Phi(1 - \eta) + \delta\rho] + \theta^2(\delta - \mu).
\end{aligned} \tag{30}$$

We remark that, by the Descartes rules, if $U_4 < 0$, there exists at least one coexistence equilibrium. In particular:

- if $\{U_3 > 0, U_4 > 0\}$, (6) does not admit any coexistence equilibrium;
- if $\{U_3 > 0, U_4 < 0\}$ or $\{U_3 < 0, U_4 < 0\}$, (6) admits a unique coexistence equilibrium;
- if $\{U_3 < 0, U_4 > 0\}$, (6) admits two coexistence equilibria.

5 Linear instability

In this Section, we investigate the linear instability of the coexistence equilibrium. In particular, we look for conditions guaranteeing the stability in the absence of diffusion and instability driven by the diffusion (Turing instability). In this analysis we show that the sign of a_{11} plays a fundamental role. In fact, $a_{11} > 0$ is a necessary condition for the occurrence of such a kind of instability.

5.1 Linear instability in the absence of diffusion

The Jacobian matrix – evaluated in E_* – is

$$\mathcal{L}^0 = \begin{pmatrix} a_{11} & a_{12} \\ a_{21} & -1 \end{pmatrix} \quad (31)$$

with

$$\begin{cases} a_{11} = -n_* + \frac{(1-\eta)^2 \sigma \Phi n_* p_*}{[1 + \sigma(1-\eta)n_* + \xi p_*]^2}, & a_{21} = \frac{\theta(1-\eta)p_*^2}{[(1-\eta)n_* + \nu]^2} > 0 \\ a_{12} = -\frac{\mu \rho n_*}{(1 + \rho n_*)^2} - \frac{[1 + \sigma(1-\eta)n_*](1-\eta)\Phi n_*}{[1 + \sigma(1-\eta)n_* + \xi p_*]^2} < 0. \end{cases} \quad (32)$$

In [18] it has been proved that $a_{11} < 0$ implies the linear stability of E_* . However, this is only a sufficient condition for the linear stability. In fact, setting

$$I_1^0 = \text{tr} \mathcal{L}^0 = a_{11} - 1, \quad I_2^0 = \det \mathcal{L}^0 = -a_{11} - a_{12} a_{21} \quad (33)$$

the characteristic equation whose solutions are the \mathcal{L}^0 -eigenvalues, is

$$\lambda^2 - I_1^0 \lambda + I_2^0 = 0. \quad (34)$$

Hence

$$a_{11} < \min\{1, -a_{12} a_{21}\}, \quad (35)$$

guarantees that $\{I_1^0 < 0, I_2^0 > 0\}$, i.e. the validity of the Routh-Hurwitz conditions necessary and sufficient to guarantee that all the roots of (34) have negative real part ([35]).

5.2 Linear instability of E^* in the presence of diffusion

Setting

$$U_1 = n - n^*, \quad U_2 = p - p^*, \quad (36)$$

the linear system governing the evolution of perturbation fields to E_* , is

$$\frac{\partial \mathbf{U}}{\partial t} = \mathcal{L}^0 \mathbf{U} + \mathcal{D} \mathbf{U}, \quad (37)$$

where $\mathbf{U} = (U_1, U_2)^T$, \mathcal{L}^0 is given by (31) and $\mathcal{D} = \begin{pmatrix} \gamma_1 & 0 \\ 0 & \gamma_2 \end{pmatrix}$. The dispersion relation governing the eigenvalues λ in terms of the wave number k is

$$\lambda^2 - T_k \lambda + h(k^2) = 0, \quad (38)$$

where

$$\begin{cases} T_k = \text{tr}(\mathcal{L}^0) - k^2 \text{tr} \mathcal{D} = I_1^0 - k^2(\gamma_1 + \gamma_2), \\ h(k^2) = \det \mathcal{D} k^4 + k^2(\gamma_1 - a_{11} \gamma_2) + \det \mathcal{L}^0 = \gamma_1 \gamma_2 k^4 + k^2(\gamma_1 - a_{11} \gamma_2) + I_2^0. \end{cases} \quad (39)$$

We remark that, if either

$$a_{11} < \min \left\{ 1, -a_{12} a_{21}, \frac{\gamma_1}{\gamma_2} \right\}, \quad (40)$$

or

$$\begin{cases} 0 < a_{11} < \min \{1, -a_{12} a_{21}\}, & \gamma_1 < a_{11} \gamma_2, \\ (\gamma_1 - a_{11} \gamma_2)^2 - 4 \gamma_1 \gamma_2 I_2^0 < 0, \end{cases} \quad (41)$$

then $T_k < 0$, $h(k^2) > 0, \forall k$, i.e. E_* – stable in the absence of diffusion – continues to be stable in the presence of diffusion too.

From (35) and (40), the condition $a_{11} < 0$ implies stability in the absence and in the presence of diffusion.

Hence, if we are looking for conditions guaranteeing the diffusion-driven instability, we have to explore the dynamics in the case $0 < a_{11} < \min\{1, -a_{12}a_{21}\}$. Since $\mathbf{I}_1^0 < 0 \Rightarrow T_k < 0, \forall k$, for the occurrence of Turing instability, it is sufficient that $h(k^2)$ assumes some negative value (i.e. its minimum is negative). In view of

$$\frac{\partial h(k^2)}{\partial k^2} = 2\gamma_1\gamma_2k^2 + \gamma_1 - a_{11}\gamma_2, \quad (42)$$

it turns out that the minimum of $h(k^2)$ is obtained for

$$(k^2)_{\min} = \frac{a_{11}\gamma_2 - \gamma_1}{2\gamma_1\gamma_2}. \quad (43)$$

From the positive definiteness of k^2 it follows that, a *necessary* condition for the occurrence of Turing instability is

$$\frac{\gamma_1}{\gamma_2} < a_{11}. \quad (44)$$

Obviously, (44) requires that $a_{11} > 0$ in order to be satisfied. The minimum of $h(k^2)$ is

$$(h(k^2))_{\min} = \mathbf{I}_2^0 - \frac{(a_{11}\gamma_2 - \gamma_1)^2}{4\gamma_1\gamma_2}. \quad (45)$$

Hence $h(k^2)$ assumes some negative value if $\mathbf{I}_2^0 < \frac{(a_{11}\gamma_2 - \gamma_1)^2}{4\gamma_1\gamma_2}$. Summarizing,

$$\begin{cases} 0 < a_{11} < \min\{1, -a_{12}a_{21}\}, & \gamma_1 < a_{11}\gamma_2, \\ \mathbf{I}_2^0 < \frac{(a_{11}\gamma_2 - \gamma_1)^2}{4\gamma_1\gamma_2}, \end{cases} \quad (46)$$

guarantees that Turing instability occurs.

To the bifurcation, $(\mathbf{I}_{2i})_{\min} = 0$. Setting $\gamma = \frac{\gamma_1}{\gamma_2}$, it turns out that the critical value of γ at the bifurcation, is

$$\gamma_c = (2\mathbf{I}_2^0 + a_{11})^2 - 2\sqrt{\mathbf{I}_2^0(\mathbf{I}_2^0 + a_{11})} \quad (47)$$

and the critical wave number is

$$k_c^2 = \frac{a_{11} - \gamma_c}{2\gamma_1}. \quad (48)$$

For $\gamma > \gamma_c$, the range of the wave number for the instability, is

$$k_-^2 < k^2 < k_+^2, \quad (49)$$

with

$$\begin{cases} k_-^2 = \frac{-(\gamma_1 - a_{11}\gamma_2) - \sqrt{\Delta}}{2\gamma_1\gamma_2}, & k_+^2 = \frac{-(\gamma_1 - a_{11}\gamma_2) + \sqrt{\Delta}}{2\gamma_1\gamma_2}, \\ \Delta = (\gamma_1 - a_{11}\gamma_2)^2 - 4\gamma_1\gamma_2\mathbf{I}_2^0. \end{cases} \quad (50)$$

Investigation shows that the set of biologically meaningful parameters verifying (46) is not empty but small. Then, in order to better explore the pattern formation in the most significant case $a_{11} < 0$, model (2) needs to be generalized. To this aim, in the following section, we investigate the influence of linear cross-diffusion terms on the population dynamics.

6 Cross-diffusion driven instability

When both linear self and cross-diffusion terms are introduced, the linear system (37) can be rewritten as follows

$$\frac{\partial \mathbf{U}}{\partial t} = \mathcal{L}^0 \mathbf{U} + \mathcal{D}' \Delta \mathbf{U}, \quad (51)$$

where

$$\mathcal{L}^0 = \begin{pmatrix} a_{11} & a_{12} \\ a_{21} & -1 \end{pmatrix}, \quad \mathcal{D}' = \begin{pmatrix} \gamma_{11} & \gamma_{12} \\ \gamma_{21} & \gamma_{22} \end{pmatrix}, \quad (52)$$

$\gamma_{11} = \gamma_1, \gamma_{22} = \gamma_2$ and $\det \mathcal{D}' > 0$. The dispersion relation (38) which gives the eigenvalue λ in terms of the wave number k is

$$\lambda^2 - \mathbf{T}'_k \lambda + \mathbf{h}'(k^2) = 0, \quad (53)$$

where

$$\begin{cases} \mathbf{T}'_k = \text{tr}(\mathcal{L}^0) - k^2 \text{tr}(\mathcal{D}') = \mathbf{I}_1^0 - k^2(\gamma_{11} + \gamma_{22}) = \mathbf{T}_k, \\ \mathbf{h}'(k^2) = \det \mathcal{D}' k^4 + q' k^2 + \det \mathcal{L}^0 = (\gamma_{11} \gamma_{22} - \gamma_{12} \gamma_{21}) k^4 + q' k^2 + \mathbf{I}_2^0, \\ q' = \gamma_{11} - a_{11} \gamma_{22} + a_{12} \gamma_{21} + a_{21} \gamma_{12}. \end{cases} \quad (54)$$

We are looking for those modes $k \neq 0$ such that $h'(k^2) < 0$. The only possibility for $h'(k^2) < 0$ is requiring $q' < 0$. The condition for the marginal stability at some $k^2 = k_{cr}^2$ is $\min(h'(k_{cr}^2)) = 0$ and the minimum of h' is reached at $k_{cr}^2 = -\frac{q'}{2 \det \mathcal{D}'}$. In addition $h'(k_{cr}^2) < 0$ gives $q'^2 - 4 \mathbf{I}_2^0 \det \mathcal{D}' > 0$.

The conditions for cross-diffusion-driven instability of system (51),(7) around the homogeneous steady state E_* can be summarized as follows

$$\begin{cases} a_{11} - 1 < 0, & -a_{11} - a_{12} a_{21} > 0, \\ a_{21} \gamma_{12} + a_{12} \gamma_{21} + \gamma_{11} - a_{11} \gamma_{22} < 0, \\ \gamma_{11} \gamma_{22} - \gamma_{12} \gamma_{21} > 0, \\ (a_{21} \gamma_{12} + a_{12} \gamma_{21} + \gamma_{11} - a_{11} \gamma_{22})^2 + 4(a_{11} + a_{12} a_{21})(\gamma_{11} \gamma_{22} - \gamma_{12} \gamma_{21}) > 0. \end{cases} \quad (55)$$

The above inequalities (55) define a region where the coexistence equilibrium E^* is unstable. Choosing γ_{12} as bifurcation parameter and $\gamma_{12} = \gamma_{12}^{cr}$ as Turing threshold, bifurcation happens at the critical value

$$\gamma_{12}^{cr} = \frac{A + \sqrt{B}}{a_{21}^2} \quad (56)$$

where

$$A = a_{21}(a_{12} \gamma_{21} + a_{11} \gamma_{22} - \gamma_{11}) + 2a_{11} \gamma_{21} \quad (57)$$

$$\begin{aligned} B = & 2a_{21}^2(-2\gamma_{11}a_{12}\gamma_{21} + a_{12}a_{11}\gamma_{21})\gamma_{22} - 2a_{11}\gamma_{11}\gamma_{22} - 2a_{12}a_{21}\gamma_{11}\gamma_{22} + 4a_{11}^2\gamma_{21}^2 \\ & - 4a_{21}(a_{11}\gamma_{11}\gamma_{21} - a_{12}a_{11}\gamma_{21}^2 - a_{11}^2\gamma_{22}\gamma_{21}) \end{aligned} \quad (58)$$

corresponding with the critical wavenumber

$$k_{cr}^2 = \sqrt{-\frac{a_{11} + a_{12} a_{21}}{\gamma_{11} \gamma_{22} - \gamma_{12} \gamma_{21}}} \neq 0 \quad (59)$$

For $\gamma_{12} > \gamma_{12}^{cr}$ the unstable wavenumbers stay in between the roots k_-^2, k_+^2 roots of $h'(k^2) = 0$.

7 Amplitude equations and stability of spatial patterns

To obtain the intervals of control parameters for different kinds of spatial patterns - which provide information on inhomogeneous distribution of both populations on the whole domain - we need to derive and analyze via multiple scale analysis the amplitude equations. The well-known amplitude equations are obtained via the standard method. Here we give the main steps. We consider the following system and take γ_{12} as a Turing bifurcation parameter

$$\begin{aligned} \begin{pmatrix} \frac{\partial n}{\partial t} \\ \frac{\partial p}{\partial t} \end{pmatrix} = & L(\gamma_{12}) \begin{pmatrix} n \\ p \end{pmatrix} + \frac{1}{2} \begin{pmatrix} f_{nn} n^2 + 2f_{np} np + f_{pp} p^2 \\ g_{nn} n^2 + 2g_{np} np + g_{pp} p^2 \end{pmatrix} \\ & + \frac{1}{6} \begin{pmatrix} f_{nnn} n^3 + 3f_{nnp} n^2 p + f_{npp} np^2 + f_{ppp} p^3 \\ g_{nnn} n^3 + 3g_{nnp} n^2 p + g_{npp} np^2 + g_{ppp} p^3 \end{pmatrix}, \end{aligned} \quad (60)$$

where we take the linear operator

$$L(\gamma_{12}) = \begin{pmatrix} a_{11} + \gamma_{11} \Delta & a_{12} + \gamma_{12} \Delta \\ a_{21} + \gamma_{21} \Delta & a_{22} + \gamma_{22} \Delta \end{pmatrix} \quad (61)$$

the expression of a_{ij} are given in (32) and

$$\begin{aligned}
f_{nn} &= -2 - \frac{-2n^2(1+an^\alpha)^3 + n^\alpha p \alpha(1-\alpha+an^\alpha(1+\alpha))}{n^2(1+an^\alpha)^3}, \quad f_{pp} = 0, \\
f_{np} &= -\frac{n^{-1+\alpha}\alpha}{(1+an^\alpha)^2}, \quad g_{pp} = g_{ppp} = g_{npp} = 0, \quad g_{np} = \frac{n^{-1+\alpha}\alpha\gamma}{(1+an^\alpha)^2}, \\
g_{nn} &= -\frac{n^{-2+\alpha}\alpha p(1-\alpha+an^\alpha(1+\alpha))\gamma}{(1+an^\alpha)^3}, \quad g_{nnn} = \frac{1}{(1+an^\alpha)^4}, \\
g_{nnp} &= \frac{n^{-2+\alpha}\alpha(1-\alpha+an^\alpha(1+\alpha))}{(1+an^\alpha)^3}, \quad f_{nnn} = -\frac{1}{(1+an^\alpha)^4}, \\
f_{ppp} &= f_{npp} = 0, \quad f_{nnp} = \frac{n^{-2+\alpha}\alpha(1-\alpha+an^\alpha(1+\alpha))}{(1+an^\alpha)^3}.
\end{aligned} \tag{62}$$

At the onset of Turing instability, the solution of our problem can be expanded

$$\mathbf{X} = \mathbf{X}_s + \sum_{j=1}^3 \mathbf{X}_0 [A_j \exp(i\mathbf{k}_j \cdot \mathbf{r}) + \bar{A}_j \exp(-i\mathbf{k}_j \cdot \mathbf{r})] \tag{63}$$

where \mathbf{X}_s represents the uniform steady state, \mathbf{X}_0 the direction of eigenmodes and A_j, \bar{A}_j the amplitudes associated with the modes $\mathbf{k}_j, -\mathbf{k}_j$. Introducing the additional small parameter ϵ , near the Turing critical value γ_{12}^{cr} , we perturb the bifurcation parameter γ_{12} along n, p, t

$$\begin{aligned}
\gamma_{12} &= \gamma_{12}^{cr} + \epsilon\gamma_{12}^{(1)} + \epsilon^2\gamma_{12}^{(2)} + \epsilon^3\gamma_{12}^{(3)} + \dots \\
n &= \epsilon n_1 + \epsilon^2 n_2 + \epsilon^3 n_3 + \dots \\
p &= \epsilon p_1 + \epsilon^2 p_2 + \epsilon^3 p_3 + \dots \\
t &= t_0 + \epsilon t_1 + \epsilon^2 t_2 + \dots
\end{aligned} \tag{64}$$

This leads to

$$L(\gamma_{12}(\epsilon)) = L^{cr} + \epsilon\gamma_{12}^{(1)} \begin{pmatrix} 0 & \Delta \\ 0 & 0 \end{pmatrix} + \epsilon^2\gamma_{12}^{(2)} \begin{pmatrix} 0 & \Delta \\ 0 & 0 \end{pmatrix} + o(\epsilon^2), \tag{65}$$

where

$$L^{cr} = \begin{pmatrix} a_{11} + \gamma_{11}\Delta & a_{12} + \gamma_{12}^{cr}\Delta \\ a_{21} + \gamma_{21}\Delta & a_{22} + \gamma_{22}\Delta \end{pmatrix}, \tag{66}$$

To apply the multiple scale method we introduce $t_0 = t, t_1 = \epsilon t, t_2 = \epsilon^2 t$, and we obtain

$$\frac{\partial}{\partial t} = \frac{\partial}{\partial t_0} + \epsilon \frac{\partial}{\partial t_1} + \epsilon^2 \frac{\partial}{\partial t_2} + o(\epsilon^2) \tag{67}$$

From (60) and balancing the coefficients of ϵ^j , we have at first order

$$L^{cr} \begin{pmatrix} n_1 \\ p_1 \end{pmatrix} = \begin{pmatrix} 0 \\ 0 \end{pmatrix} \tag{68}$$

at second order

$$\begin{aligned}
L^{cr} \begin{pmatrix} n_2 \\ p_2 \end{pmatrix} &= \frac{\partial}{\partial t_1} \begin{pmatrix} n_1 \\ p_1 \end{pmatrix} - \begin{pmatrix} 0 & \gamma_{12}^{(1)} \\ 0 & 0 \end{pmatrix} \begin{pmatrix} n_1 \\ p_1 \end{pmatrix} + \Delta \begin{pmatrix} n_1 \\ p_1 \end{pmatrix} \\
&\quad - \frac{1}{2} \begin{pmatrix} f_{nn}n_1^2 + 2f_{np}n_1p_1 + f_{pp}p_1^2 \\ g_{nn}n_1^2 + 2g_{np}n_1p_1 + g_{pp}p_1^2 \end{pmatrix} = \begin{pmatrix} F_n \\ F_p \end{pmatrix}
\end{aligned} \tag{69}$$

at third order

$$\begin{aligned}
L^{cr} \begin{pmatrix} n_3 \\ p_3 \end{pmatrix} &= \begin{pmatrix} \frac{\partial n_2}{\partial t_1} + \frac{\partial n_1}{\partial t_2} \\ \frac{\partial p_2}{\partial t_1} + \frac{\partial p_1}{\partial t_2} \end{pmatrix} - \begin{pmatrix} 0 & \gamma_{12}^{(1)} \\ 0 & 0 \end{pmatrix} \Delta \begin{pmatrix} n_2 \\ p_2 \end{pmatrix} - \begin{pmatrix} 0 & \gamma_{12}^{(1)} \\ 0 & 0 \end{pmatrix} \Delta \begin{pmatrix} n_1 \\ p_1 \end{pmatrix} \\
&\quad - \begin{pmatrix} f_{nn}n_1n_2 + f_{np}(n_1p_2 + n_2p_1) + f_{pp}p_1p_2 \\ g_{nn}n_1n_2 + g_{np}(n_1p_2 + n_2p_1) + g_{pp}p_1p_2 \end{pmatrix} \\
&\quad - \frac{1}{6} \begin{pmatrix} f_{nnn}n_1^3 + 3f_{nnp}n_1^2p_1 + 3f_{npp}n_1p_1^2 + f_{ppp}p_1^3 \\ g_{nnn}n_1^3 + 3g_{nnp}n_1^2p_1 + 3g_{npp}n_1p_1^2 + g_{ppp}p_1^3 \end{pmatrix} = \begin{pmatrix} G_n \\ G_p \end{pmatrix}
\end{aligned} \tag{70}$$

Solving (68) we obtain

$$\begin{pmatrix} n_1 \\ p_1 \end{pmatrix} = \begin{pmatrix} \phi \\ 1 \end{pmatrix} \left(\sum_{j=1}^3 W_j \exp(i\mathbf{k}_j \cdot \mathbf{r}) + c.c. \right), \quad (71)$$

where c.c. denotes the complex conjugate of the previous terms, W_j is the amplitude of the mode $\exp(i\mathbf{k}_j \cdot \mathbf{r})$ ($j=1,2,3$) and $\phi = \frac{a_{12} - \gamma_{12}^{cr} k_{cr}^2}{\gamma_{11} k_{cr}^2 - a_{11}}$.

According to the Fredholm solvability condition, the functions of the right-hand side of (69) must be orthogonal to the eigenvectors of the zero eigenvalue of \bar{L}_T which is the adjoint operator of L_T . The eigenvectors of the operator \bar{L}_T are $\begin{pmatrix} 1 \\ \psi \end{pmatrix} \exp(-i\mathbf{k}_j \cdot \mathbf{r}) + c.c. (j = 1, 2, 3)$ with $\psi = \frac{a_{12} - \gamma_{12}^{cr} k_{cr}^2}{\gamma_{22} k_{cr}^2 + 1}$.

The orthogonality condition is

$$(1, \psi) \begin{pmatrix} F_n^j \\ F_p^j \end{pmatrix} = 0, \quad (j = 1, 2, 3)$$

where F_n^j and F_p^j give the coefficients of $\exp(i\mathbf{k}_j \cdot \mathbf{r})$ in F_n and F_p . From this relation it follows

$$\begin{cases} (\phi + \psi) \frac{\partial W_1}{\partial t_1} = -k_{cr}^2 \gamma_{12}^{(1)} W_1 + (f_2 + \psi g_2) \bar{W}_2 \bar{W}_3, \\ (\phi + \psi) \frac{\partial W_2}{\partial t_1} = -k_{cr}^2 \gamma_{12}^{(1)} W_2 + (f_2 + \psi g_2) \bar{W}_3 \bar{W}_1, \\ (\phi + \psi) \frac{\partial W_3}{\partial t_1} = -k_{cr}^2 \gamma_{12}^{(1)} W_3 + (f_2 + \psi g_2) \bar{W}_1 \bar{W}_2, \end{cases} \quad (72)$$

where

$$\begin{cases} f_2 = f_{nn} \phi^2 + 2f_{np} \phi + f_{pp}, \\ g_2 = g_{nn} \phi^2 + 2g_{np} \phi + g_{pp}. \end{cases} \quad (73)$$

Following a similar procedure for (69) its solution will be of type

$$\begin{aligned} \begin{pmatrix} n_2 \\ p_2 \end{pmatrix} &= \begin{pmatrix} N_0 \\ P_0 \end{pmatrix} + \sum_{j=1}^3 \begin{pmatrix} N_j \\ P_j \end{pmatrix} \exp(i\mathbf{k}_j \cdot \mathbf{r}) + \sum_{j=1}^3 \begin{pmatrix} N_{jj} \\ P_{jj} \end{pmatrix} \exp(2i\mathbf{k}_j \cdot \mathbf{r}) \\ &+ \sum_{j=1}^3 \begin{pmatrix} N_{12} \\ P_{12} \end{pmatrix} \exp(i(\mathbf{k}_1 - \mathbf{k}_2) \cdot \mathbf{r}) + \sum_{j=1}^3 \begin{pmatrix} N_{23} \\ P_{23} \end{pmatrix} \exp(i(\mathbf{k}_2 - \mathbf{k}_3) \cdot \mathbf{r}) \\ &+ \sum_{j=1}^3 \begin{pmatrix} N_{31} \\ P_{31} \end{pmatrix} \exp(i(\mathbf{k}_3 - \mathbf{k}_1) \cdot \mathbf{r}) + c.c. \end{aligned} \quad (74)$$

Substituting in (69), separating the coefficients of $\exp(0)$, $\exp(i\mathbf{k}_j \cdot \mathbf{r})$, $\exp(2i\mathbf{k}_j \cdot \mathbf{r})$, $\exp(i(\mathbf{k}_1 - \mathbf{k}_2) \cdot \mathbf{r})$ (and permuting the suffixes we obtain also the coefficients corresponding to $\exp(i(\mathbf{k}_2 - \mathbf{k}_3) \cdot \mathbf{r})$, $\exp(i(\mathbf{k}_3 - \mathbf{k}_1) \cdot \mathbf{r})$) denoting by

$$\mathcal{M}_k = \begin{pmatrix} a_{11} - \gamma_{11} k^2 & a_{12} - \gamma_{12}^{cr} k^2 \\ a_{21} - \gamma_{21} k^2 & -1 - \gamma_{22} k^2 \end{pmatrix} \quad (75)$$

we get, for $N_j = \phi P_j$, $j = 1, 2, 3$

$$\begin{aligned} \begin{pmatrix} N_0 \\ P_0 \end{pmatrix} &= \mathcal{M}_0^{-1} \begin{pmatrix} -f_2 \\ -g_2 \end{pmatrix} (|W_1|^2 + |W_2|^2 + |W_3|^2) = \begin{pmatrix} Z_{n0} \\ Z_{p0} \end{pmatrix} (|W_1|^2 + |W_2|^2 + |W_3|^2), \\ \begin{pmatrix} N_{11} \\ P_{11} \end{pmatrix} &= \mathcal{M}_{2k_{cr}}^{-1} \begin{pmatrix} -\frac{f_2}{2} \\ -\frac{g_2}{2} \end{pmatrix} W_1^2 = \begin{pmatrix} Z_{n1} \\ Z_{p1} \end{pmatrix} W_1^2, \\ \begin{pmatrix} N_{12} \\ P_{12} \end{pmatrix} &= \mathcal{M}_{\sqrt{3}k_{cr}}^{-1} \begin{pmatrix} -f_2 \\ -g_2 \end{pmatrix} W_1 \bar{W}_2 = \begin{pmatrix} Z_{n2} \\ Z_{p2} \end{pmatrix} W_1 \bar{W}_2. \end{aligned}$$

At third order, collecting the coefficients $(G_n^1, G_p^1)^T$ of $\exp(i\mathbf{k}_1 \cdot \mathbf{r})$ from (70), we find

$$\begin{pmatrix} G_n^1 \\ G_p^1 \end{pmatrix} = \begin{pmatrix} \phi \left(\frac{\partial P_1}{\partial t_1} + \frac{\partial W_1}{\partial t_2} \right) \\ \frac{\partial P_1}{\partial t_1} + \frac{\partial W_1}{\partial t_2} \end{pmatrix} - \begin{pmatrix} 0 & \gamma_{12}^{(1)} \\ 0 & 0 \end{pmatrix} \begin{pmatrix} \phi P_1 \\ -k_{cr}^2 P_1 \end{pmatrix} - \begin{pmatrix} 0 & \gamma_{12}^{(2)} \\ 0 & 0 \end{pmatrix} \begin{pmatrix} \phi W_1 \\ -k_{cr}^2 W_1 \end{pmatrix}$$

$$\begin{aligned}
& - \left(\begin{aligned} & [(f_{nn}\phi + f_{np})(Z_{n0} + Z_{n1}) + (f_{np}\phi + f_{pp})(Z_{p0} + Z_{p1})]|W_1|^2 + [(f_{nn}\phi + f_{np})(Z_{n0} + Z_{n2}) \\ & + (f_{np}\phi + f_{pp})(Z_{p0} + Z_{p2})](|W_2|^2 + |W_3|^2)]W_1 + f_2(\bar{W}_2\bar{P}_3 + \bar{W}_3\bar{P}_2) \\ & ((g_{nn}\phi + g_{np})(Z_{n0} + Z_{n1}) + (g_{np}\phi + g_{pp})(Z_{p0} + Z_{p1})]|W_1|^2 + [(g_{nn}\phi + g_{np})(Z_{n0} + Z_{n2}) \\ & + (g_{np}\phi + g_{pp})(Z_{p0} + Z_{p2})](|W_2|^2 + |W_3|^2)]W_1 + g_2(\bar{W}_2\bar{P}_3 + \bar{W}_3\bar{P}_2) \end{aligned} \right) \\
& - \left(\begin{aligned} & (|W_1|^2 + |W_2|^2 + |W_3|^2)(f_{nnn}\phi^3 + 3f_{nnp}\phi^2 + 3f_{npp}\phi + f_{ppp}) \\ & (|W_1|^2 + |W_2|^2 + |W_3|^2)(g_{nnn}\phi^3 + 3g_{nnp}\phi^2 + 3g_{npp}\phi + g_{ppp}) \end{aligned} \right) W_1 \quad (76)
\end{aligned}$$

Analogously, permutating the subscript of W and P , we can find the other coefficients $(G_n^2, G_p^2)^T$, $(G_n^3, G_p^3)^T$.

From Fredholm solvability condition $(1, \psi) \begin{pmatrix} G_n^j \\ G_p^j \end{pmatrix} = 0$, $j = 1, 2, 3$ it follows that

$$\begin{cases} (\phi + \psi) \left(\frac{\partial W_1}{\partial t_2} + \frac{\partial P_1}{\partial t_1} \right) = -k_{cr}^2 (\gamma_{12}^{(1)} P_1 + \gamma_{12}^{(2)} W_1) \\ \quad + h_1 (\bar{W}_2 \bar{P}_3 + \bar{W}_3 \bar{P}_2) - (G_1 |W_1|^2 + G_2 (|W_2|^2 + |W_3|^2)) W_1 \\ (\phi + \psi) \left(\frac{\partial W_2}{\partial t_2} + \frac{\partial P_2}{\partial t_1} \right) = -k_{cr}^2 (\gamma_{12}^{(1)} P_2 + \gamma_{12}^{(2)} W_2) \\ \quad + h_1 (\bar{W}_3 \bar{P}_1 + \bar{W}_1 \bar{P}_3) - (G_1 |W_2|^2 + G_2 (|W_3|^2 + |W_1|^2)) W_2 \\ (\phi + \psi) \left(\frac{\partial W_3}{\partial t_2} + \frac{\partial P_3}{\partial t_1} \right) = -k_{cr}^2 (\gamma_{12}^{(1)} P_3 + \gamma_{12}^{(2)} W_3) \\ \quad + h_1 (\bar{W}_1 \bar{P}_2 + \bar{W}_2 \bar{P}_1) - (G_1 |W_3|^2 + G_2 (|W_1|^2 + |W_2|^2)) W_3 \end{cases} \quad (77)$$

with

$$\begin{aligned} h_1 &= f_2 + \psi g_2 \\ G_1 &= -[(f_{nn}\phi + f_{np} + \psi(g_{nn}\phi + g_{np})) (Z_{n0} + Z_{n1}) \\ & \quad + (f_{np}\phi + f_{pp} + \psi(g_{np}\phi + g_{pp})) (Z_{p0} + Z_{p1})] + f_3 + \psi g_3 \\ G_2 &= -[(f_{nn}\phi + f_{np} + \psi(g_{nn}\phi + g_{np})) (Z_{n0} + Z_{n2}) \\ & \quad + (f_{np}\phi + f_{pp} + \psi(g_{np}\phi + g_{pp})) (Z_{p0} + Z_{p2})] + f_3 + \psi g_3 \\ f_3 &= f_{nnn}\phi^3 + 3f_{nnp}\phi^2 + 3f_{npp}\phi + f_{ppp} \\ g_3 &= g_{nnn}\phi^3 + 3g_{nnp}\phi^2 + 3g_{npp}\phi + g_{ppp} \end{aligned} \quad (78)$$

Denoting by A_j the amplitude and expanding as follows

$$A_j = \epsilon W_j + \epsilon^2 V_j + o(\epsilon^2)$$

from

$$\frac{\partial A_j}{\partial t} = \epsilon \frac{\partial A_j}{\partial t_1} + \epsilon^2 \frac{\partial A_j}{\partial t_2} + o(\epsilon^2). \quad (79)$$

we obtain the amplitude equations

$$\begin{cases} \tau_0 \frac{\partial A_1}{\partial t} = \mu A_1 + h \bar{A}_2 \bar{A}_3 - (b_1 |A_1|^2 + b_2 (|A_2|^2 + |A_3|^2)) A_1 \\ \tau_0 \frac{\partial A_2}{\partial t} = \mu A_2 + h \bar{A}_3 \bar{A}_1 - (b_1 |A_2|^2 + b_2 (|A_3|^2 + |A_1|^2)) A_2 \\ \tau_0 \frac{\partial A_3}{\partial t} = \mu A_3 + h \bar{A}_1 \bar{A}_2 - (b_1 |A_3|^2 + b_2 (|A_1|^2 + |A_2|^2)) A_3 \end{cases} \quad (80)$$

where

$$\tau_0 = -\frac{(\phi + \psi)}{k_{cr}^2 \gamma_{12}^{cr}}, \quad \mu = \frac{\gamma_{12} - \gamma_{12}^{cr}}{\gamma_{12}^{cr}}, \quad h = -\frac{h_1}{k_{cr}^2 \gamma_{12}^{cr}}, \quad b_1 = -\frac{G_1}{k_{cr}^2 \gamma_{12}^{cr}}, \quad b_2 = -\frac{G_2}{k_{cr}^2 \gamma_{12}^{cr}}$$

Each amplitude can be expressed through a mode $\rho_j = |A_j|$ and a corresponding phase angle θ_j as $A_j = \rho_j \exp(i\theta_j)$, $j = 1, 2, 3$. Substituting in (80) and separating the real and imaginary parts we obtain

$$\begin{cases} \tau_0 \frac{\partial \theta}{\partial t} = -h \frac{\rho_1^2 \rho_2^2 + \rho_1^2 \rho_3^2 + \rho_2^2 \rho_3^2}{\rho_1 \rho_2 \rho_3} \sin \theta \\ \tau_0 \frac{\partial \rho_1}{\partial t} = \mu \rho_1 + h \rho_2 \rho_3 \cos \theta - b_1 \rho_1^3 - b_2 (\rho_2^2 + \rho_3^2) \rho_1 \\ \tau_0 \frac{\partial \rho_2}{\partial t} = \mu \rho_2 + h \rho_3 \rho_1 \cos \theta - b_1 \rho_2^3 - b_2 (\rho_3^2 + \rho_1^2) \rho_2 \\ \tau_0 \frac{\partial \rho_3}{\partial t} = \mu \rho_3 + h \rho_1 \rho_2 \cos \theta - b_1 \rho_3^3 - b_2 (\rho_1^2 + \rho_2^2) \rho_3 \end{cases} \quad (81)$$

with $\theta = \theta_1 + \theta_2 + \theta_3$. The above dynamical system admits the following different kinds of solutions:

Parameters	δ	ϕ	σ	ξ	θ	ν	η
Values	0.5	2	2	3	0.95	0.1	0.2

Table 1: Fixed values for some model parameters

- The homogeneous stationary state represented by

$$\rho_1 = \rho_2 = \rho_3 = 0 \quad (82)$$

which is stable for $\mu < \mu_2 = 0$ and unstable for $\mu > \mu_2 = 0$.

- Stripe pattern represented by

$$\rho_1 = \sqrt{\frac{\mu}{b_1}} \neq 0, \quad \rho_2 = \rho_3 = 0, \quad (83)$$

which are stable for $b_1 < b_2$ and $\mu > \mu_3 = \frac{b_1 h^2}{(b_2 - b_1)^2}$.

- Hexagonal pattern represented by

$$\rho_1 = \rho_2 = \rho_3 = \rho_H^\pm = \frac{|h| \pm \sqrt{h^2 + 4(b_1 + 2b_2)\mu}}{2(b_1 + 2b_2)}; \quad (84)$$

which exist and are stable when $2(b_1 + 2b_2) > 0$ and $\mu > \mu_H = -\frac{h^2}{4(b_1 + 2b_2)}$. Therefore, the hexagons

for $\rho_H = \rho_H^+$ are stable if $\mu < \mu_{H2} = \frac{(2b_1 + b_2)h^2}{(b_2 - b_1)^2}$, while for the solution $\rho_H = \rho_H^-$ the hexagonal structures are unstable.

- Mixed state given by

$$\rho_1 = \frac{|h|}{b_2 - b_1}, \quad \rho_2 = \rho_3 = \sqrt{\frac{\mu - b_1 \rho_1^2}{b_1 + b_2}} \quad (85)$$

with $\mu > b_1 \rho_1^2$ and $b_2 > b_1$ and is always unstable.

8 Numerical Simulations

In order to evaluate the effect of cross diffusion, we have assigned a constant value to many of model parameters (as reported in Table 1), we fixed values to $\gamma_{11}, \gamma_{21}, \gamma_{22}$ and assumed γ_{12} as a bifurcation parameter. According to (56), it is possible to determine γ_{12}^{cr} as the minimum value for Turing instability to occur. Fig. 1 represents the plots of $h'(k^2)$ as defined in (54)₂ for different values of the bifurcation parameter γ_{12} . In this specific example, we have assumed $\gamma_{11} = 3, \gamma_{21} = 11, \gamma_{22} = 4$ so that it is $\gamma_{12}^{cr} \approx 1.0748$. In addition from (55)₄ it is possible to estimate an upper value $\gamma_{12}^{up} \approx 1.0909$ above which the condition (55)₄ is no longer satisfied and from (55)₅ a lower value $\gamma_{12}^{low} \approx 1.0748$ above which (55)₅ is satisfied. In the right panel of the same figure, a zoom of the same plots is shown. As can be seen, for $\gamma_{12} < 1.0748$ the curve does not intersect the horizontal axis, so that there are not unstable modes. As γ_{12} increases, the range of unstable modes increases as well. Similarly, as the bifurcation parameter increases, the real part of the corresponding eigenvalue becomes positive (see Fig. 2).

We also investigate the effect of the fear level and prey refuge on the unstable modes. As shown in Fig. 3, once the parameter γ_{12} is fixed we can notice that higher values of the fear level ρ lead to smaller regions of unstable modes. For this reason, as it will be shown in the following experiments, the main effects of a lower fear level are to accelerate the insurgence of patterns and to increase the instability of the system, when the chosen γ_{12} is quite far from its value γ_{12}^{low} .

In Fig. 4 it has been shown that for fixed values of γ_{12} it can be noticed that higher values of the prey refuge η lead to larger regions of unstable modes. In addition, higher values of the prey refuge level imply the increase of the instability and the acceleration of the insurgence of patterns when the chosen γ_{12} is quite far from its value γ_{12}^{low} .

In the rest of this section we perform some numerical simulations for system (51) on a two dimensional spatial domain, illustrating the final stable patterns for the prey and predator population for different values

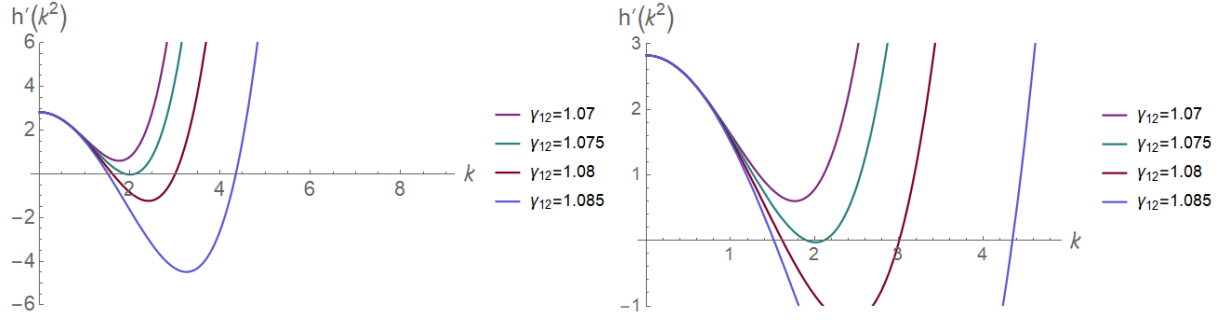


Figure 1: Left panel: plots of $h'(k^2)$ as a function of the wavenumber k for different values of the bifurcation parameter γ_{12} ; in the right panel, a detail of the same plots. Here $\gamma_{11} = 3$, $\gamma_{21} = 11$, $\gamma_{22} = 4$, and other parameter values as in Table 1

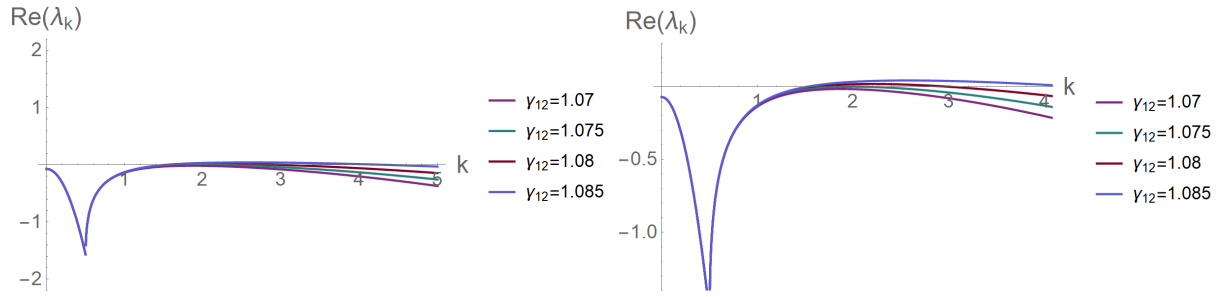


Figure 2: Left panel: plots of the real part of the eigenvalue λ , solution of (53), as a function of the wavenumber k for different values of the bifurcation parameter γ_{12} ; in the right panel, a detail of the same plots. Here again $\gamma_{11} = 3$, $\gamma_{21} = 11$, $\gamma_{22} = 4$, and other parameter values as in Table 1

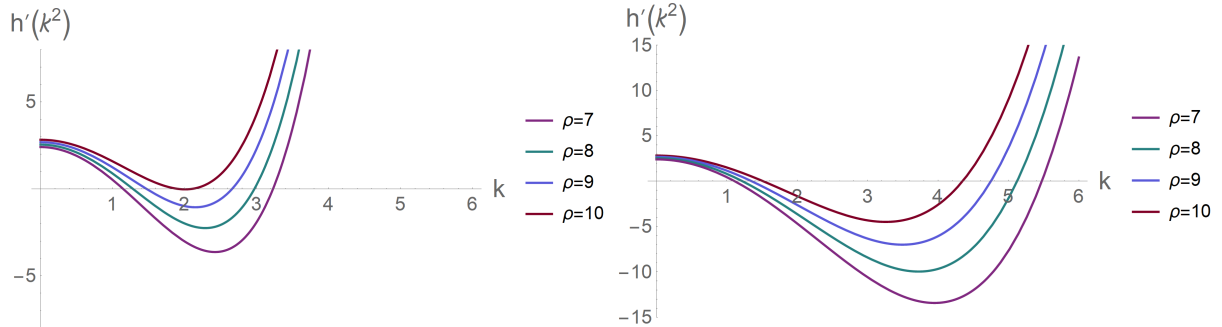


Figure 3: Plots of $h'(k^2)$ as a function of the wavenumber k for different values of the fear level ρ and $\gamma_{11} = 3$; $\gamma_{22} = 4$, $\gamma_{21} = 11$. In the left panel, $\gamma_{12} = 1.075$; in the right panel $\gamma_{12} = 1.085$. The other parameter values as in Table 1

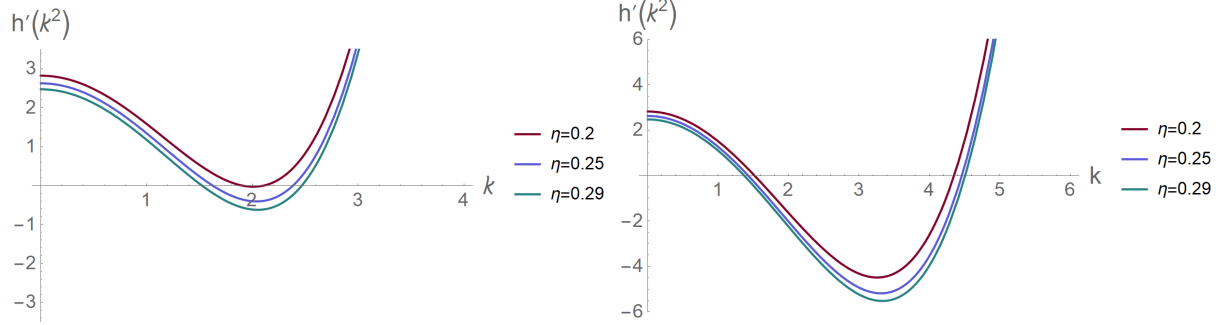


Figure 4: Plots of $h'(k^2)$ as a function of the wavenumber k for different values of the prey refuge level η and $\gamma_{11} = 3$; $\gamma_{22} = 4$, $\gamma_{21} = 11$. In the left panel, $\gamma_{12} = 1.075$; in the right panel $\gamma_{12} = 1.085$. The other parameter values as in Table 1

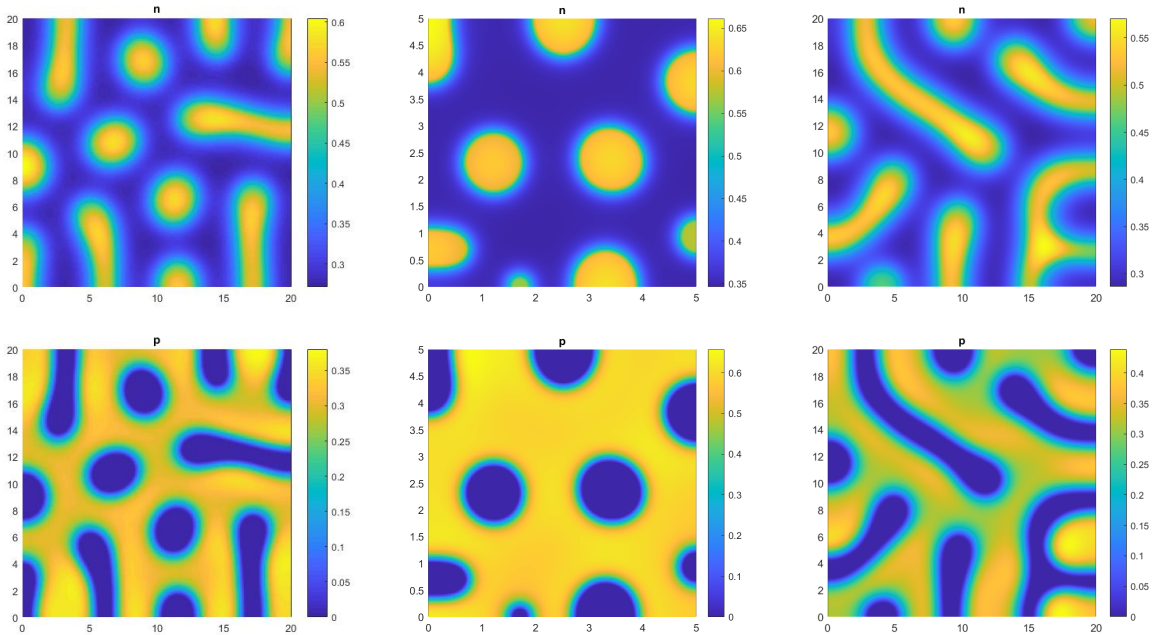


Figure 5: Snapshot of pattern formation for different values of diffusion coefficients and $\rho = 10$. First column: prey and predator population distribution for $\mu = 2$, $\gamma_{11} = 3$, $\gamma_{22} = 4$, $\gamma_{21} = 13$, $\gamma_{12} = 0.6915$. Second column: prey and predator population distribution for $\mu = 3$, $\gamma_{11} = 3$, $\gamma_{22} = 4$, $\gamma_{21} = 11$, $\gamma_{12} = 1.08$. Third column: prey and predator population distribution for $\mu = 2$, $\gamma_{11} = 4$, $\gamma_{22} = 4$, $\gamma_{21} = 15.5$, $\gamma_{12} = 0.7735$. All the other parameter values as in Table 1.

of diffusion coefficients. The numerical simulations are performed by using, for the spatial discretization, the finite difference method with step $\Delta h = 0.025$ (for a domain $[0, 5] \times [0, 5]$) and $\Delta h = 0.1$ (for a domain $[0, 20] \times [0, 20]$) while for the time discretization, the explicit Euler's method, with time step $\Delta t = 10^{-6}$. For different values of diffusion coefficients satisfying the Turing conditions, we have obtained different types of Turing patterns representing the distribution of prey and predator species. In every pattern the blue color corresponds to the low density of species and the yellow color corresponds to the high density of species. By various numerical simulations we have observed that prey are distributed generating predominantly spot patterns. Biologically, yellow spots on the blue background represent that the prey population disposes in isolated regions with high density, moved by fear to better defend themselves from predation. Precisely, as shown in the columns of Fig. 5, representing from up to bottom the prey and predator distribution respectively, hexagonal structures (corresponding to spots), spots and stripes, for prey, appear. The numerical simulations are well consistent with the theoretical analysis results of amplitude equations.

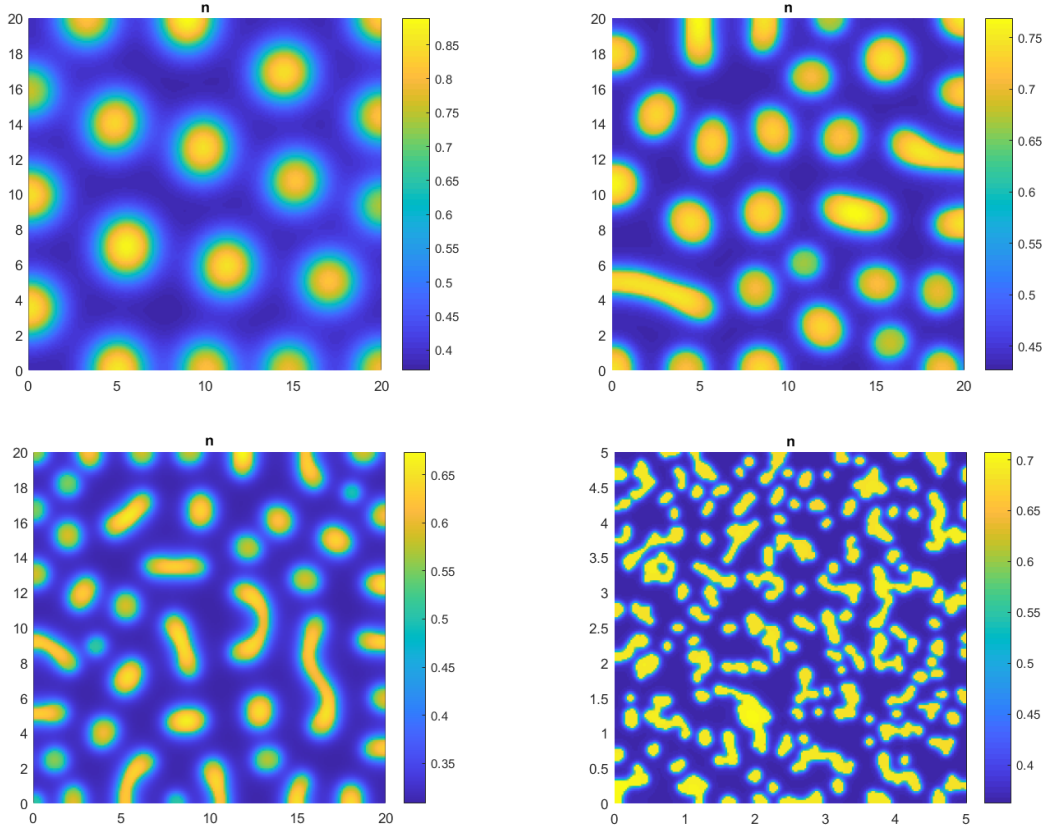


Figure 6: Snapshot of pattern formation for prey for different values of fear and diffusion coefficients. First row, from left to right: $(\rho = 5, \eta = 0.1, \gamma_{11} = 4, \gamma_{12} = 0.77, \gamma_{22} = 3, \gamma_{21} = 15.5)$; $(\rho = 5, \eta = 0.1, \gamma_{11} = 6, \gamma_{12} = 1.11, \gamma_{22} = 3, \gamma_{21} = 15.5)$. Second row, from left to right: $(\rho = 15, \eta = 0.4, \gamma_{11} = 2, \gamma_{12} = 0.65, \gamma_{22} = 3.5, \gamma_{21} = 15.5)$; $(\rho = 18, \eta = 0.5, \gamma_{11} = 2, \gamma_{12} = 0.99, \gamma_{22} = 5, \gamma_{21} = 10)$. $\mu = 3$ and other parameter values as in Table 1.

Figure 6 depicts stable patterns of prey distribution, emerging by choosing the value of ρ and η and consequently the value of diffusion coefficients (satisfying (55)) representing the following scenario. Precisely, the first and second images represent the distribution of prey population, with a low level of both fear and refuge ($\rho = 5, \eta = 0.1$), which is therefore more tempted to spread in the domain, in search of food and consequently subject to high predatory pressure ($\gamma_{11} = 4, \gamma_{12} = 0.77, \gamma_{21} = 15.57, \gamma_{22} = 3$ and $\gamma_{11} = 6, \gamma_{12} = 1.11, \gamma_{21} = 15.57, \gamma_{22} = 3$ respectively). The third and fourth images represent the prey distribution characterized by a higher level of fear and refuge ($\rho = 15, \eta = 0.4$ and $\rho = 18, \eta = 0.5$ respectively) which is therefore less likely to spread to the environment ($\gamma_{11} = 2, \gamma_{12} = 0.65, \gamma_{22} = 3.5, \gamma_{21} = 15.5$ and $\gamma_{11} = 2, \gamma_{12} = 0.99, \gamma_{22} = 5, \gamma_{21} = 10$).

9 Conclusions

In this paper, a generalized Leslie-Gower model is introduced to describe the interaction between prey and predator populations. In particular, a random movement of both the species is allowed: at the first, a simple self diffusion is considered for both the species and, after, the more general case in which the diffusion of one species depends on the movement of the other species, is analyzed (cross-diffusion system). A qualitative analysis concerning the boundedness of solutions, existence of absorbing sets in the phase space, the non-existence of non constant steady state, is performed. The linear instability analysis of the coexistence equilibrium (when it exists) is investigated. In particular, conditions guaranteeing self-diffusion and cross-diffusion induced instability, have been determined. Numerical simulations on the obtained results are shown. In particular, by varying the values of the model parameters, Turing patterns emerged, representing

a spatial redistribution of population in the environment. These results may have wide applications in ecology, biological control for the coexistence of the species in the ecosystem.

Declarations

- **Funding** No funding has been received for this article
- **Conflict of interest** We declare we have no competing interest
- **Ethics approval** Not applicable
- **Consent to participate** Not applicable
- **Consent for publication** All authors gave final approval for publication and agree to be held accountable for the work performed therein
- **Availability of data and materials** This article has no additional data
- **Code availability** Not applicable
- **Authors' contributions** The authors have equally contributed to each part of this paper. They conceived and thoroughly discussed the main ideas, mathematical models and results of this paper by mutual consent. All of them carried out in detail the proofs and calculations

Acknowledgments

This paper has been performed under the auspices of the GNFM of INdAM.

References

- [1] F. Capone, R. De Luca, and S. Rionero. On the stability of non-autonomous perturbed lotka-volterra models. *Applied Mathematics and Computation*, 219(12):6868–6881, 2013.
- [2] F. Capone, MF. Carfora, R. De Luca, and I. Torcicollo. On the dynamics of an intraguild predator–prey model. *Math Comput Simulation.*, 149:17–31, 2018.
- [3] F. Capone, M. F. Carfora, R. De Luca, and I. Torcicollo. Turing patterns in a reaction-diffusion system modeling hunting cooperation. *Math Comput Simulation*, 165:172–180, 2019.
- [4] F. Capone, M. F. Carfora, R. De Luca, and I. Torcicollo. Nonlinear stability and numerical simulations for a reaction–diffusion system modelling Allee effect on predators. *International Journal of Nonlinear Sciences and Numerical Simulation*, 23(5):751–760, 2022.
- [5] M. F. Carfora and I. Torcicollo. Cross-diffusion-driven instability in a predator-prey system with fear and group defense. *Mathematics*, 8(8):1244, 2020.
- [6] B.D. Dalziel, E. Thomann, J. Medlock, and P. De Leenheer. Global analysis of a predator–prey model with variable predator search rate. *Journal of Mathematical Biology*, 81:159–183, 2020.
- [7] R. De Luca. On the long-time dynamics of nonautonomous predator-prey models with mutual interference. *Ricerche di Matematica*, 61(2):275–290, 2012.
- [8] S. Deeptajyoti, S. Ghorai, M. Banerjee, and A. Morozov. Bifurcation analysis of the predator–prey model with the Allee effect in the predator. *Journal of Mathematical Biology*, 84(7), 2022.
- [9] J.D. Murray. *Mathematical Biology I. An Introduction*, volume 17. Interdisciplinary Applied Mathematics; Springer: New York, NY, USA, Springer edition, 2002.
- [10] J.D. Murray. *Mathematical Biology II: Spatial Models and Biomedical Applications*, volume 18. Interdisciplinary Applied Mathematics; Springer: New York, NY, USA, Springer edition, 2003.
- [11] F. Chen, L. Chen, and X. Xie. On a Leslie–Gower predator–prey model incorporating a prey refuge. *Nonlinear Analysis: Real World Applications*, 10(5):2905–2908, 2009.
- [12] S. Yu. Global stability of a modified Leslie-Gower model with Beddington-DeAngelis functional response. *Advances in Difference Equations*, 2014(1):1–14, 2014.
- [13] R. Gupta and P. Chandra. Bifurcation analysis of modified Leslie–Gower predator–prey model with Michaelis–Menten type prey harvesting. *Journal of Mathematical Analysis and Applications*, 398(1):278–295, 2013.

-
- [14] A. Korobeinikov. A Lyapunov function for Leslie-Gower predator-prey models. *Applied Mathematics Letters*, 14:697–699, 2001.
- [15] C. Holling. The functional response of predators to prey density and its role in mimicry and population regulation. *The Memoirs of the Entomological Society of Canada*, 97(S45):5–60, 1965.
- [16] J. R. Beddington. Mutual interference between parasites or predators and its effect on searching efficiency. *J. Animal Ecol.*, 44:331–340, 1975.
- [17] D.L. DeAngelis, R. A. Goldstein, and R.V. O’Neill. A model for trophic interaction. *Ecology*, 56:881–892, 1975.
- [18] A. L. Firdiansyah. Effect of fear in Leslie-Gower predator-prey model with Beddington-DeAngelis functional response incorporating prey refuge. *International Journal of Computing Science and Applied Mathematics*, 7(2):56–62, 2021.
- [19] W. Cresswell. Predation in bird populations. *Journal of Ornithology*, 152(1):251–263, 2011.
- [20] X. Wang, L. Zanette, and X. Zou. Modelling the fear effect in predator–prey interactions. *J. Math. Biol.*, 73:1179–1204, 2016.
- [21] Y. Huang, Z. Zhu, and Z. Li. Modeling the Allee effect and fear effect in predator–prey system incorporating a prey refuge. *Advances in Difference Equations*, 2020(321), 2020.
- [22] Z. Zhu, R. Wu, L. Lai, and X. Yu. The influence of fear effect to the Lotka–Volterra predator–prey system with predator has other food resource. *Advances in Difference Equations*, 2020(237), 2020.
- [23] J. Ghosh, B. Sahoo, and S. Poria. Prey-predator dynamics with prey refuge providing additional food to predator. *Chaos, Solitons & Fractals*, 96:110–119, 2017.
- [24] A. Sih. Prey refuges and predator-prey stability. *Theoretical Population Biology*, 31(1):1–12, 1987.
- [25] A. A. Thirthar, S. J. Majeed, M. A. Alqudah, P. Panja, and T. Abdeljawad. Fear effect in a predator-prey model with additional food, prey refuge and harvesting on super predator. *Chaos, Solitons & Fractals*, 159:1–12, 2022.
- [26] R. S. Cantrell and C. Cosner. *Spatial ecology via reaction-diffusion equations*. John Wiley and Sons Ltd., 2003.
- [27] A. M. Turing. The Chemical Basis for Morphogenesis. *Philos. Trans. R. Soc. Lond. Ser. B, Biol. Sci.*, 237:37–72, 1952.
- [28] I. Torricollo. On the nonlinear stability of a continuous duopoly model with constant conjectural variation. *Int J Non-Linear Mech*, 81:268–273, 2016.
- [29] S. Rionero and I. Torricollo. On the dynamics of a nonlinear reaction-diffusion duopoly model. *Int J Non-Linear Mech*, 99:105–111, 2018.
- [30] M. F. Carfora and I. Torricollo. Identification of epidemiological models: the case study of yemen cholera outbreak. *Applicable Analysis*, 101(10):3744–3754, 2020.
- [31] A. R. M. Jamil and R. K. Naji. Modeling and analysis of the influence of fear on the harvested modified Leslie-Gower model involving nonlinear prey refuge. *Mathematics*, 10(16), 2022.
- [32] H. Chen and C. Zhang. Dynamic analysis of a Leslie–Gower-type predator–prey system with the fear effect and ratio-dependent Holling III functional response. *Nonlinear Analysis: Modelling and Control*, 27(5):1244, 2022.
- [33] L. Dung. Dissipativity and global attractors for a class of quasilinear parabolic systems. *Commun. Partial Diff. Eqns.*, 22:213–433, 1997.
- [34] J. Flavin and S. Rionero. *Qualitative Estimates for Partial Differential Equations: An Introduction*. Boca Raton, CRC Press Inc. edition, 1996.
- [35] D.R. Merkin. *Introduction to the theory of stability*, volume 24. Springer, Text in Applied Mathematics, 1997.